Journal of The Electrochemical Society, **146** (3) 908-913 (1999)
S0013-4651(98)07-009-8 CCC: $7.00

$LiNi_xCu_{0.5-x}Mn_{1.5}O_4$ Spinel Electrodes, Superior High-Potential Cathode Materials for Li Batteries

I. Electrochemical and Structural Studies

Yair Ein-Eli,[a,*,d] John T. Vaughey,[b] Michael M. Thackeray,[b,*] Sanjeev Mukerjee,[c,*] Xiao Q. Yang,[*,c] and James McBreen[c,*]

[a]*Covalent Associates, Incorporated, Woburn, Massachusettes 01801, USA*
[b]*Argonne National Laboratory, Argonne, Illinois 60439, USA*
[c]*Brookhaven National Laboratory, Upton, New York 11973-5000, USA*

$LiNi_xCu_{0.5-x}Mn_{1.5}O_4$ ($0 \le x \le 0.5$) spinel materials that are of interest as electrodes for lithium-ion batteries have been studied by crystallographic and electrochemical methods. Electrochemical results show that the inclusion of Ni into the Cu-modified spinel increases the overall reversible capacity from 72 mAh/g with $LiCu_{0.5}Mn_{1.5}O_4$ ($x = 0$) at 4.95 V to 120 mAh/g with $LiNi_{0.5}Mn_{1.5}O_4$ ($x = 0.5$) at 4.6 V. The Cu-rich spinels in the $LiNi_xCu_{0.5-x}Mn_{1.5}O_4$ system show enhanced stability upon cycling. These spinel products are difficult to prepare in single-phase form. Neutron diffraction data show that the end members $LiNi_{0.5}Mn_{1.5}O_4$ and $LiCu_{0.5}Mn_{1.5}O_4$ contain small amounts of lithium-nickel-oxide and lithium-copper-oxide impurity phases, respectively; these impurities affect the composition of the spinel component. The composition of the spinel component in $LiNi_{0.5}Mn_{1.5}O_4$ was determined from a combined X-ray and neutron diffraction profile refinement to be $Li_{0.97}Ni_{0.42}Mn_{1.61}O_4$.

Manuscript submitted July 6, 1998; revised manuscript received October 6, 1998.

Over the last 30 years, transition metal oxides and chalcogenides have been used as cathode (positive eletrode) materials in primary and rechargeable Li batteries.[1-3] The shift in the emphasis of research and development to "Li-ion" batteries (that use host structures for Li at both the anode and cathode) has occurred because of the inability of a pure Li electrode to offer safe operation and long cycle life. In order to achieve a high energy density in Li-ion cells, it has been necessary to use cathode materials such as $LiMO_2$ (M = Ni, Co)[4,5] or $LiMn_2O_4$ [6] ($0 \le x \le 1$), which provide potentials of approximately 4 V vs. metallic Li. Currently, $LiCoO_2$ is the cathode material of choice for lithium-ion batteries; this cathode was commercialized first by Sony Corporation.[7]

During the past four years, several research groups have aimed their work at the development of cathode materials with "ultrahigh" potential, typically those that offer a voltage between 4 and 5.1 V vs. Li.[8-12] For example, Guyomard and co-workers[9] showed that lithium extraction from a Cr-substituted spinel, $LiCr_xMn_{2-x}O_4$ occurs by a two-step process at 4 and 4.9 V. These reactions were attributed to the oxidation of Mn and Cr ions, respectively. Gao et al.[10] discovered that lithium extraction from $LiNi_{0.5}Mn_{1.5}O_4$ occurs at a potential of 4.6-4.7 V. They attributed this reaction to the oxidation of Ni^{2+} to Ni^{4+}. Recently we reported the electrochemical behavior of Cu-substituted spinels, $LiCu_xMn_{2-x}O_4$ ($0.1 \le x \le 0.5$).[11,12] These materials show a reversible electrochemical reaction at 4.95 V, attributed to the oxidation/reduction of Cu^{2+}/Cu^{3+}. [13]

In this paper we report the synthesis of spinel electrodes in the $LiNi_xCu_{0.5-x}Mn_{1.5}O_4$ system ($0 \le x \le 0.5$), as well as their structural and electrochemical evaluation. Although $LiNi_{0.5}Mn_{1.5}O_4$ ($x = 0.5$) offers a high capacity (up to 120 mAh/g, similar to the practical capacity obtained from unmodified Mn spinel cathode material) at high potential (4.6-4.7 V),[10] it shows limited stability upon cycling; on the other hand, $LiCu_{0.5}Mn_{1.5}O_4$ ($x = 0$) offers a relatively stable cycle life but is limited by a low reversible capacity of approximately 70 mAh/g. [11,12] Our intention was to synthesize a group of materials that would have synergetic features of both end members. For that purpose we aimed this research at the synthesis of novel cathode materials within the composition range $0 \le x \le 0.5$ in the $LiNi_xCu_{0.5-x}Mn_{1.5}O_4$ system. We also examined in detail the structure of the $LiNi_{0.5}Mn_{1.5}O_4$ end member by X-ray and neutron diffraction analysis, as we did previously with $LiCu_{0.5}Mn_{1.5}O_4$. [12] The data provide a much better understanding of the electrochemical behavior of $LiNi_{0.5}Mn_{1.5}O_4$ than reported previously.[10] Structural features are used to explain the electrochemical behavior of $LiNi_{0.5}Mn_{1.5}O_4$ electrodes.

Experimental

$LiNi_xCu_{0.5-x}Mn_{1.5}O_4$ cathode materials were prepared by a sol-gel process in which stoichiometric amounts of CH_3COOLi (Acros), $Ni(OOCH_3)_2$ (Alfa), $Cu(OOCH_3)_2$ (Alfa), and $Mn(OOCH_3)_2$ (Aldrich) were dissolved in a mixture of deionized water and ethanol (1:1 v/v). The mixtures were stirred with gentle heating (80°C) for 4 h, and NH_4OH (28-30%, J. T. Baker) was added to the mixture until a gel was formed. The mixtures were then heated to dryness on a rotary evaporator and, thereafter, were ground into a powder. The powdered precursors were heated for 12 h in air at 500°C, subsequently refired at 650°C (12 h), and finally calcined at 750°C for another 12 h. Elemental analysis, undertaken by Laboratory Testing (Dublin, PA), confirmed the composition of the final products.

Rigaku DMAX/2200V (Cu Kα) and Philips 1840 diffractometers (Fe Kα) were used to obtain powder X-ray diffraction patterns to characterize the samples. For the detailed structural analysis of $LiNi_{0.5}Mn_{1.5}O_4$, X-ray diffraction data were collected on an automated Siemens D5000 diffractometer with Cu Kα radiation. Neutron data were collected on the General Purpose Powder Diffractometer at the Intense Pulsed Neutron Source at Argonne National Laboratory.

Cyclic voltammograms of $LiNi_xCu_{0.5-x}Mn_{1.5}O_4$ electrodes were obtained and recorded at a slow sweep rate of 15 μV/s (EG&G/Princeton Applied Research potentiostat, model 263A). Lithium metal served as both counter and reference electrodes.

Cycling data were collected on Starbuck multichannel cyclers. $LiNi_xCu_{0.5-x}Mn_{1.5}O_4$ cathode materials were studied in cells with a Li foil anode (10 mil, Cyprus Foote Mineral) separated by Whatman BS-65 glass microfibers in a 1 cm^2 parallel-plate configuration. Cathode films were prepared from slurries of $LiCu_xNi_{0.5-x}Mn_{1.5}O_4$ with 10% polyvinylidene difluoride (PVDF, Atochem, North America) and 10% (w/w) carbon black (super S) dissolved in *N*-methyl-2-pyrrolidinone (NMP, Aldrich). The mixtures were cast (doctor-bladed) onto Al foil, dried at 120°C under vacuum for 2 h, then roll-compressed at 100 atm, resulting in the formation of cathode films containing 5-6 mg/cm^2 of active material. Cell assembly was carried out under an Ar atmosphere. For cycle-life tests, cells were cycled between potential limits of 3.3 and 5.1 V at a current density of 250 μA/cm^2.

The electrolyte composition was 1 M $LiPF_6$ (Hashimoto Chemicals) in a mixture of ethylene carbonate (EC, EM Industries) and

* Electrochemical Society Active Member.
[d] Current address: Electric Fuel, Limited, Bet Shemesh 99000, Israel.

S0013-4651(98)07-009-8 CCC: $7.00

ethyl methyl carbonate (EMC, Covalent Associates, Inc.) in a volume ratio of 1 EC:3 EMC. Cells were charged and discharged galvanostatically at a current density of 0.25 mA/cm^2 within the potential limits of 3.3-5.1 V.

Results and Discussion

Structural Characterization.—X-ray diffraction patterns of $LiNi_xCu_{0.5-x}Mn_{1.5}O_4$ samples.—The X-ray diffraction patterns of $LiNi_{0.25}Cu_{0.25}Mn_{1.5}O_4$ prepared via the described sol-gel method are shown in Fig. 1. Refiring at 650°C resulted in the incorporation of most of the unreacted manganese oxides into the spinel structure. However, a final 750°C soak was needed in order to complete the reaction; only traces of MnO_x impurities are present in the diffraction patterns, as shown in Fig. 1. Figure 2 shows the XRD patterns of $LiNi_xCu_{0.5-x}Mn_{1.5}O_4$ samples for $x = 0$ (pattern A), $x = 0.25$ (pattern B), and $x = 0.5$ (pattern C). All the cathode materials exhibit a cubic spinel structure. Whereas pattern A ($LiCu_{0.5}Mn_{1.5}O_4$) shows no detectable impurity, patterns B ($LiCu_{0.25}Ni_{0.25}Mn_{1.5}O_4$) and C ($LiNi_{0.5}Mn_{1.5}O_4$) show evidence of small, but significant, impurities. These impurities were attributed to trace amounts of MnO_x (also observable in Fig. 1), Li_2MnO_3, and a lithium-nickel-oxide phase. On the basis of the XRD patterns, we believe that incorporation of Ni into the spinel lattice is more difficult to accomplish than the incorporation of copper. The XRD patterns also indicate that as the Ni content in $LiNi_xCu_{0.5-x}Mn_{1.5}O_4$ increases, the peak positions shift to a higher scattering angle, indicating a decrease in the lattice parameter of the cubic unit cell. Figure 3 shows the variation in unit cell dimension as a function of x in $LiNi_xCu_{0.5-x}Mn_{1.5}O_4$. The lattice parameter of the $LiNi_xCu_{0.5-x}Mn_{1.5}O_4$ structure increases with decreasing x, from 8.1551(1) for $x = 0.5$ through 8.1635(1) for $x = 0.25$ to 8.1967(1) for $x = 0$.

X-ray diffraction analysis of $LiNi_{0.5}Mn_{1.5}O_4$.—A combined X-ray and neutron-diffraction study of a product with the composition of the end member $LiCu_{0.5}Mn_{1.5}O_4$ ($x = 0$) has been reported previously.[12] The refinement showed that the product had two phases and that the composition of the spinel component was $Li_{1.01}Cu_{0.32}Mn_{1.67}O_4$. Therefore, in this study we have concentrated our efforts on refining the other end member of the $LiNi_xCu_{0.5-x}Mn_{1.5}O_4$, namely, $LiNi_{0.5}Mn_{1.5}O_4$ ($x = 0.5$).

The initial structure refinement of the spinel component with XRD data reflected the ideal composition, $Li[Ni_{0.5}Mn_{1.5}]O_4$, despite the presence of a small amount of a lithium nickel oxide ($Li_xNi_{1-x}O$) impurity in the sample. Because Mn and Ni have similar X-ray scattering factors, these ions could not be distinguished on the B sites of the structure. Because it was unlikely that Mn ions would occupy the tetrahedral sites, a subsequent refinement was carried out to determine whether there was any Ni on the A sites. The occupancy of the A site was refined to accommodate both Li and Ni, and the sum of the Li and Ni ions on each A site was constrained to unity. This refinement showed that the A sites contained 2.7% Ni. The final R and Rw factors for this refinement were 9.5 and 14.5, respectively. The results of the X-ray refinement of the spinel phase are provided in Table I. A semiquantitative analysis of the XRD pattern showed that the percentage of the lithium nickel oxide impurity phase was 1.9%. The impurity phase could be indexed to a hexagonal (rhombohedral) unit cell with lattice constants $a = 2.935(7)$ and $c = 7.982(7)$, or alternatively, to a pseudocubic unit cell with $a = 4.1516(7)$. Because pure NiO has a hexagonal (rhombohedral) unit cell with lattice constants $a \approx 2.95$, $c \approx 7.75$ (or a pseudocubic lattice constant $a \approx 4.172$), we concluded that the impurity belonged to the $Li_xNi_{1-x}O$ solid-solution system with $x \approx 0.05$ (based on the 1.9% impurity-phase content). This is consistent with data reported by Johnston and co-workers.[14]

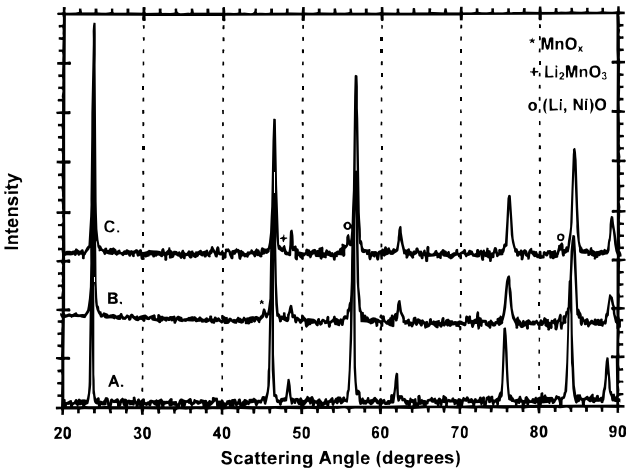

Figure 2. XRD patterns of $LiNi_xCu_{0.5-x}Mn_{1.5}O_4$ prepared via the sol-gel method. Pattern A, $x = 0$; pattern B, $x = 0.25$; pattern C, $x = 0.5$.

Neutron diffraction analysis of $LiNi_{0.5}Mn_{1.5}O_4$.—The neutron diffraction pattern of a sample with nominal composition $LiNi_{0.5}Mn_{1.5}O_4$ showed three distinct phases: (*i*) a dominant spinel phase, (*ii*) a rock-salt $Li_xNi_{1-x}O$ phase, and (*iii*) an unidentified phase. Refining the A sites of the spinel component with only lithium showed a large isotropic temperature factor ($B \approx 2.5$ ^{2}), indicating the possibility that some nickel might occupy the A-sites. In subsequent refinements, both Li and Ni were allowed to occupy the A

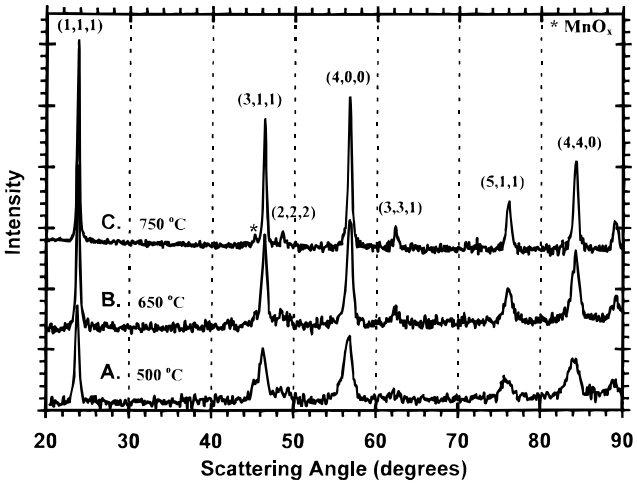

Figure 1. XRD patterns of $LiNi_{0.25}Cu_{0.25}Mn_{1.5}O_4$ prepared via the sol-gel method with calcining temperature of 500°C, followed by refiring at 650 and 750°C.

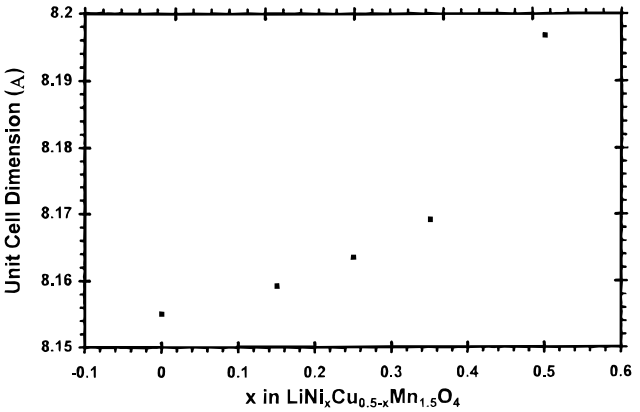

Figure 3. Cubic cell dimension for $LiNi_xCu_{0.5-x}Mn_{1.5}O_4$ as a function of x ($x = 0.5, 0.35, 0.25, 0.15, 0$).

S0013-4651(98)07-009-8 CCC: $7.00

Table I. Crystallographic parameters of the spinel component in $LiMn_{1.5}Ni_{0.5}O_4$ from X-ray data. [Space group *Fd*3*m*, *a* = 8.1633(3) Å; vol = 544.01(4) Å^3.]

Atom	Wyckoff notation	*x*	*y*	*z*	*B* (×100)	Site occupancy, *n*
Li (1)	8a	0.125	0.125	0.125	0.6 (5)	0.973 (5)
Ni (1)	8a	0.125	0.125	0.125	0.6 (5)	0.027 (5)
Mn (1)	16d	0.5	0.5	0.5	0.97 (4)	0.764 (3)
Ni (2)	16d	0.5	0.5	0.5	0.97 (4)	0.236 (3)
O (2)	32e	0.2623 (3)	0.2623 (3)	0.2623 (3)	1.3 (1)	1

Table II. Crystallographic parameters of the spinel component in $LiMn_{1.5}Ni_{0.5}O_4$ from X-ray and neutron data. (Space group *Fd*3*m*, *a* = 8.1632(4) Å; vol = 544.59(4) Å^3.)

Atom	Wyckoff notation	*x*	*y*	*z*	*B* (×100)	Site occupancy, *n*
Li (1)	8a	0.125	0.125	0.125	0.5 (2)	0.973
Ni (1)	8a	0.125	0.125	0.125	0.5 (2)	0.027
Mn (1)	16d	0.5	0.5	0.5	0.3 (3)	0.806 (4)
Ni (2)	16d	0.5	0.5	0.5	0.3 (3)	0.194 (4)
O (2)	32e	0.2623 (3)	0.2623 (3)	0.2623 (3)	0.47 (4)	1

sites while constraining the total occupancy to unity. The results indicated a small amount of Ni on these sites, thereby confirming the X-ray refinement. For the final neutron-diffraction refinements, the amount of Ni on the A sites of the spinel phase was fixed at 2.7%, the value obtained from the X-ray data. These refinements yielded a meaningful value for the thermal parameter of the A-site Li/Ni ions (0.5 ^{2}). Because Ni is a strong (negative) scatterer of neutrons (1.03×10^{-12} cm), and because Mn has a neutron scattering length of opposite sign (-0.37×10^{-12} cm), it was possible to obtain a good estimation of the relative amounts of these ions on the octahedral B sites of the spinel structure. The refinements yielded a Mn:Ni ratio on the B sites of approximately 80:20, similar to the ratio obtained for the Mn:Cu ratio in the refinement of the copper analogue.[12] Because of the difficulties associated with refining more than two atom types on one crystallographically independent site, we could not estimate the amount of lithium on the B sites; nevertheless, from the similarity of the XRD patterns of the nickel and copper spinel phases in $LiNi_{0.5}Mn_{1.5}O_4$ and $LiCu_{0.5}Mn_{1.5}O_4$ materials, we believe that the amount of Li on the B sites of the Ni spinel phase would be small (<5%) and, if present, would only marginally change the composition of the spinel phase. On this basis, the overall composition of the spinel phase in the $LiNi_{0.5}Mn_{1.5}O_4$ sample was determined to be $Li_{0.97}Ni_{0.42}Mn_{1.61}O_4$, or in spinel notation $(Li_{0.97}Ni_{0.03})_{8a}[Mn_{1.61}Ni_{0.39}]_{16d}O_4$ (Table II).

A quantitative analysis of the sample showed that the concentration of the $Li_xNi_{1-x}O$ rock-salt phase was approximately 2.1%, in excellent agreement with the results from the X-ray refinement. The lattice parameters of the $Li_xNi_{1-x}O$ phase refined were indexed to a hexagonal (rhombohedral) unit cell with lattice constants a = 2.932(1) and c = 7.972(6), also in excellent agreement with the X-ray data. The final R and Rw values were 6.06 and 8.32, respectively. If the third phase was subtracted from the pattern, the refinement yielded R values that were approximately 2% lower.

Assuming that all the Ni ions present in the spinel phase $Li_{0.97}Ni_{0.42}Mn_{1.61}O_4$ are divalent, which would be consistent with earlier studies of $LiNi_{0.5}Mn_{1.5}O_4$ samples,[10,15] the oxidation state

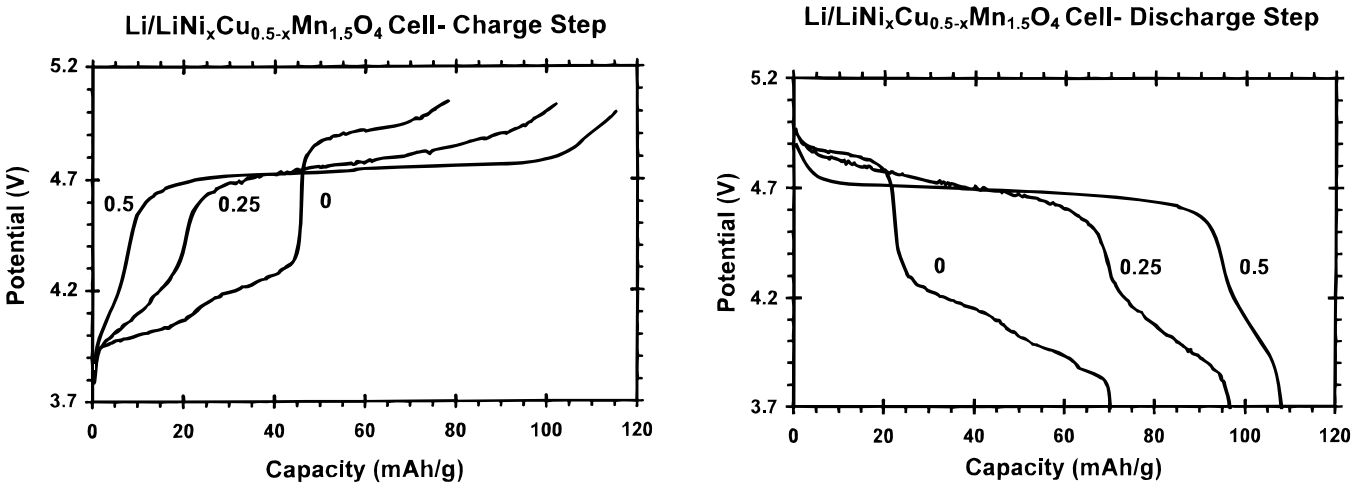

Figure 4. The potential vs. capacity curves obtained from $LiNi_xCu_{0.5-x}Mn_{1.5}O_4$ (x = 0.5, 0.25, 0) in the (a) third charge and (b) third discharge. Lithium metal served as a counter electrode in 1 M $LiPF_6$/ EMC(3):EC(1) electrolyte.

S0013-4651(98)07-009-8 CCC: $7.00

Table III. Specific capacities from Li/LiNi$_x$Cu$_{0.5-x}$Mn$_{1.5}$O$_4$ cells.

Cathode material	Potential plateaus (V)		Discharge capacity (mAh/g)		
	Lower	Upper	Total	Lower potential	Upper potential
$LiCu_{0.5}Mn_{1.5}O_4$	4.15	4.9	71	47	24
$LiNi_{0.15}Cu_{0.35}Mn_{1.5}O_4$	4.1	4.8	75	25	50
$LiCu_{0.25}Ni_{0.25}Mn_{1.5}O_4$	4.1	4.75	100	21	79
$LiNi_{0.35}Cu_{0.15}Mn_{1.5}O_4$	4.1	4.7	104	17	87
$LiNi_{0.5}Mn_{1.5}O_4$	4.1	4.6	117	12	105

of the Mn ions is 3.87. This value is slightly higher than the value of 3.80 in the spinel component $Li_{1.01}Cu_{0.32}Mn_{1.67}O_4$ of a $LiCu_{0.5}Mn_{1.5}O_4$ sample.[12]

Electrochemical studies.—Figure 4 shows the potential vs. capacity profiles obtained from the third charge (Fig. 4a) and subsequent discharge (Fig. 4b) of Li/LiNi$_x$Cu$_{0.5-x}$Mn$_{1.5}$O$_4$ cells (x = 0.5, 0.25, 0). The potential limits for the electrochemical cycling were 3.3-5.1 V; the current density was 0.25 mA/cm^2. Table III summarizes the relative capacities obtained from LiNi$_x$Cu$_{0.5-x}$Mn$_{1.5}$O$_4$ electrodes (x = 0.5, 0.35, 0.25, 0.15, 0) in the high-potential region (4.5-5.1 V) and the low-potential region (3.3-4.5 V). Figure 5 shows the cyclic voltammograms of LiNi$_x$Cu$_{0.5-x}$Mn$_{1.5}$O$_4$ electrodes obtained against a metallic Li reference electrode. Figure 5a shows voltammograms for the low-potential range (3.3-4.5 V), whereas Fig. 5b shows voltammograms for the high-potential region (4.5-5.2 V).

The overall picture that emerges from these studies is the following

1. The inclusion of Ni in LiNi$_x$Cu$_{0.5-x}$Mn$_{1.5}$O$_4$ spinel electrodes lowers the potential of the high-voltage plateau in $LiCu_{0.5}Mn_{1.5}O_4$. That is, the one-electron reaction that is associated with the oxidation reaction $Cu^{2+} \rightarrow Cu^{3+}$ in $LiCu_{0.5}Mn_{1.5}O_4$ occurs at a potential of 4.95 V, whereas the assumed two-electron process in the $Ni^{2+} \rightarrow Ni^{4+}$ transition occurs at a potential of 4.6 V. Electrodes that fall within the LiNi$_x$Cu$_{0.5-x}$Mn$_{1.5}$O$_4$ solid solution ($0 < x < 0.5$) exhibit intermediate potentials, 4.7-4.8 V, as can be seen clearly in the cyclic voltammograms of Fig. 5b.

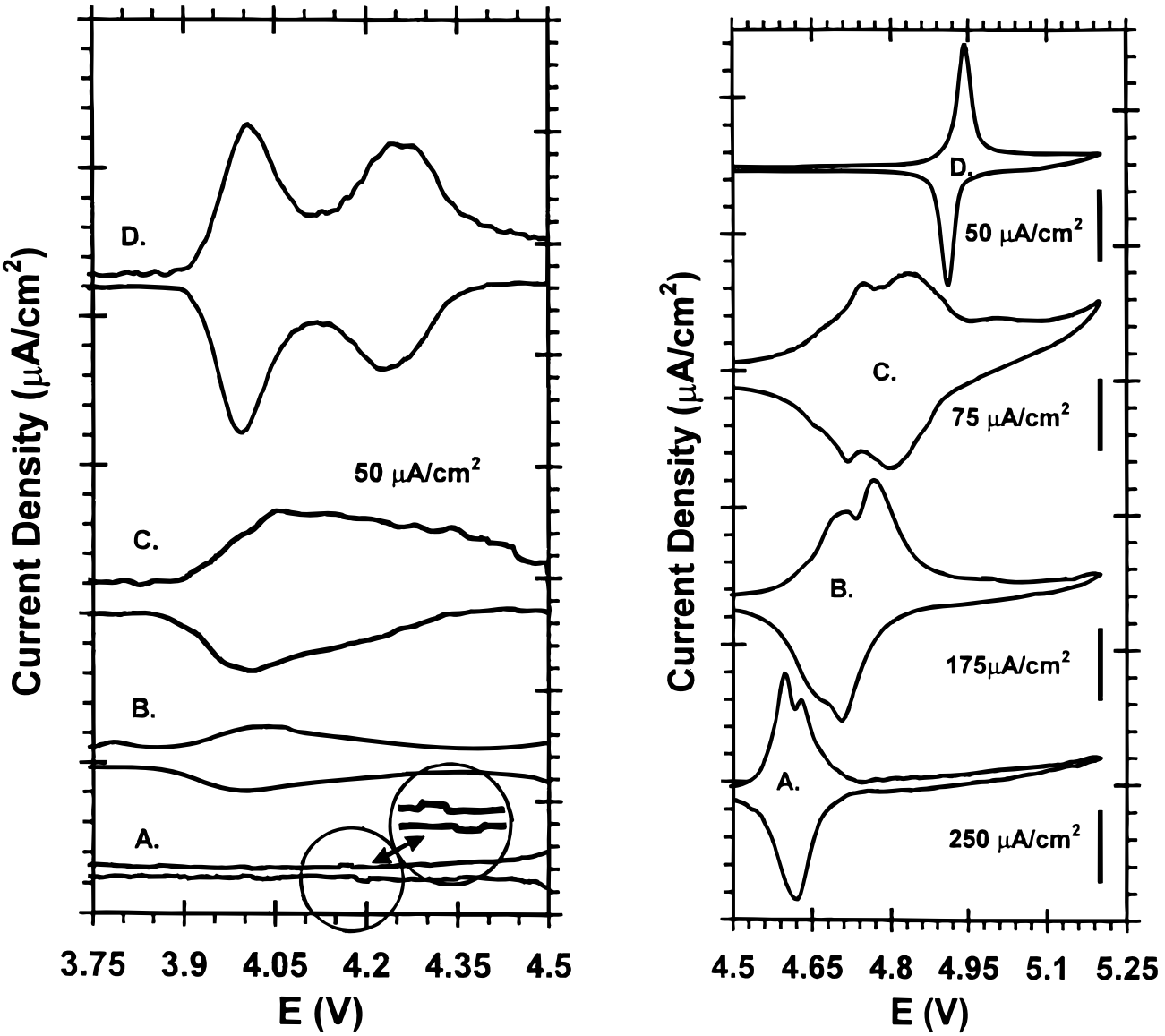

Figure 5. Cyclic voltammograms obtained from LiNi$_x$Cu0$_{.5-x}$Mn$_{1.5}$O$_4$ [x = (A) 0.5, (B) 0.35, (C) 0.15, and (D) 0] cycled within the potential limits of (a) 3.3-4.5 V and (b) 4.5-5.2 V. Lithium metal served both as counter and reference electrodes in 1 M LiPF$_6$/EMC(3):EC(1) electrolyte. Scan rate = 15 μV/s.

S0013-4651(98)07-009-8 CCC: $7.00

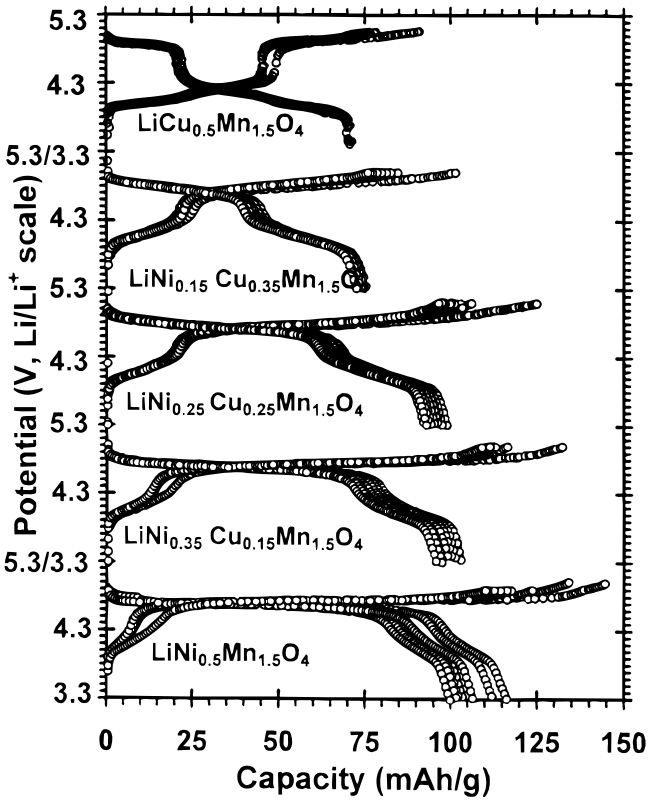

Figure 6. The potential vs. capacity profiles obtained from cycling of $LiNi_xCu_{0.5-x}Mn_{1.5}O_4$ cells (x = 0.5, 0.35, 0.25, 0.15, 0). Lithium metal served as counter electrode in 1 M $LiPF_6$/EMC(3):EC(1) electrolyte.

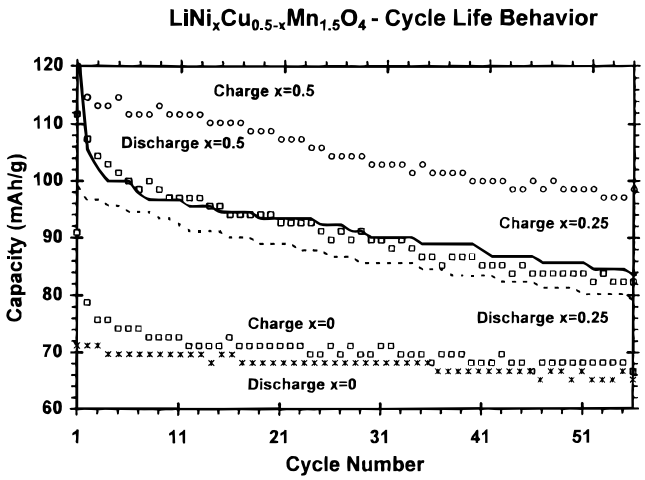

Figure 7. The cycle life behavior of $LiNi_xCu_{0.5-x}Mn_{1.5}O_4$ cells (x = 0.5, 0.25, 0). Lithium metal served as a counter electrode in 1 M $LiPF_6$/EMC(3):EC(1) electrolyte.

2. Increasing the Ni content in the spinel structure reduces the capacity of the low-potential plateau (3.3-4.5 V) and increases the capacity of the high-voltage plateau (4.5-5.2 V) (Fig. 6, Table III). However, the capacity obtained at the lower voltage range, which is related to the reversible reaction of $Mn^{3+} \rightarrow Mn^{4+}$, is not totally eliminated. The electrochemical results for the spinel electrode with the highest Ni content are consistent with the composition of the spinel component in the $LiNi_{0.5}Mn_{1.5}O_4$ sample, in which the average oxidation state of the manganese ions is 3.87. These data show that not all the Mn ions in "$LiNi_{0.5}Mn_{1.5}O_4$" samples are tetravalent, in contrast to data on similar materials reported previously by Amine et al.[15] and Gao et al.[10]

3. As x in $LiNi_xCu_{0.5-x}Mn_{1.5}O_4$ increases (Table III), the capacity obtained at the low potential (3.3-4.5 V) reduces from 47 mAh/g in $LiCu_{0.5}Mn_{1.5}O_4$ (x = 0) to 12 mAh/g in $LiNi_{0.5}Mn_{1.5}O_4$ (x = 0.5). Conversely, the capacity obtained at the high-potential plateau (4.5-5.1 V) increases from 24 mAh/g in $LiCu_{0.5}Mn_{1.5}O_4$ (x = 0), through 79 mAh/g in $LiCu_{0.25}Ni_{0.25}Mn_{1.5}O_4$ (x = 0.25), to 105 mAh/g in $LiNi_{0.5}Mn_{1.5}O_4$ (x = 0.5).

4. The overall capacity obtained from the Ni-rich spinel compounds is higher than that observed from the Cu-rich spinels. The increase in capacity can be attributed to two factors: (*i*) The two-electron process, $Ni^{2+} \rightarrow Ni^{4+}$, occurs at 4.6-4.7 V, [10] whereas Cu-ion oxidation at 4.95 V ($Cu^{2+} \rightarrow Cu^{3+}$) is a one-electron process.[14] (*ii*) Nickel is accommodated in the spinel structure, particularly on the B sites, in higher concentration than is Cu. The structural analyses have shown that in the spinel component, $(Li_{0.97}Ni_{0.03})_{8a}[Mn_{1.61}Ni_{0.39}]_{16d}O_4$, of the $LiNi_{0.5}Mn_{1.5}O_4$ sample, 19.5% of the Mn ions on the B sites are replaced by Ni ions. This replacement is higher than the Cu substitution in the $LiCu_{0.5}Mn_{1.5}O_4$ sample in which the spinel phase has the cation arrangement $(Li_{0.9}Cu_{0.1})_{8a}[Mn_{1.67}Cu_{0.22}Li_{0.11}]_{16d}O_4$, and reflects only an 11% substitution of Mn by Cu. [12]

Cycle life stability.—Figure 6 shows the potential vs. capacity plots obtained from $LiNi_xCu_{0.5-x}Mn_{1.5}O_4$ (x = 0.5, 0.35, 0.25, 0.15, 0) cells for the first ten cycles. Figure 7 shows the cycle life behavior of three $LiNi_xCu_{0.5-x}Mn_{1.5}O_4$ cells (x = 0.5, 0.25, 0). The results are surprising: although the Cu-rich spinels operate at higher voltage (4.95 V) than the Ni-rich spinels (4.6-4.7 V) and are thus more highly oxidizing materials, they are still significantly more stable to electrochemical cycling than the nickel-rich electrodes. Figure 7 illustrates that the coulombic efficiency of cells with Cu-rich electrodes, as reflected by the relatively small difference in capacity between charge and discharge cycles, is significantly better than it is in cells with Ni-rich electrodes. The large capacity difference observed in cells with Ni-rich electrodes is believed to be due to electrolyte oxidation, thus accounting for their relatively rapid capacity fade on cycling. The enhanced stability from the Cu-rich electrodes may also be attributed to the fact that they are not as deeply discharged as the Ni-rich electrodes.

Conclusions

Novel electroactive $LiNi_xCu_{0.5-x}Mn_{1.5}O_4$ spinel electrodes have been prepared and evaluated in Li cells. The data show that Li can be extracted from the spinel structures in two main potential regions: 3.9-4.3 and 4.6-5.1 V. The upper voltage is dependent on the value of x; that is, as the Ni content increases, the potential plateau decreases from 4.95 to 4.6 V. At the same time, the reversible capacity increases from approximately 72 mAh/g (x = 0) to approximately 120 mAh/g (x = 0.5). However, the Cu-rich spinel electrodes are significantly more stable to electrochemical cycling than the Ni-rich electrodes. This work has emphasized the difficulty of completely substituting manganese by other transition metals in $LiMn_{2-x}M_xO_4$ spinel compounds. A structural analysis of a nickel-rich sample with the nominal composition $LiNi_{0.5}Mn_{1.5}O_4$ shows that the sample has two phases and that the cation distribution in the spinel component, $Li_{0.97}Ni_{0.42}Mn_{1.61}O_4$, is complex but similar to that obtained previously from a structural analysis of the spinel component in a copper-rich sample of nominal composition $LiCu_{0.05}Mn_{1.5}O_4$.

In situ X-ray absorption near-edge spectroscopy (XANES) and XRD analyses of these novel materials are in progress and will be reported elsewhere.

Acknowledgments

This work was performed under an SBIR Phase II DoD program sponsored by the U.S. Army CECOM, administered by the Army Research Laboratory, Fort Monmouth, NJ, under contract no. DAAB07-97-C-D320. Support from Argonne National Laboratory and from the U.S. Department of Energy's Advanced Battery Pro-

S0013-4651(98)07-009-8 CCC: $7.00

gram, Chemical Sciences Division, Office of Basic Energy Sciences, under contract no. W-31-109-Eng-38, is gratefully acknowledged.

Covalent Associates, Incorporated, assisted in meeting the publication costs of this article.

References

1. L. Holleck and J. P. Driscoll, *Electrochim. Acta*, **22**, 647 (1977).
2. M. S. Whittingham, *Prog. Solid State Chem.*, **12**, 41 (1978).
3. M. S. Whittingham, *J. Solid State Chem.*, **29**, 303 (1979).
4. M. G. S. R. Thomas, W. I. F. David, J. B. Goodenough, and P. Groves, *MRS Bull.*, **20**, 1137 (1985).
5. K. Mizushima, P. C. Jones, P. J. Wiseman, and J. B. Goodenough, *MRS Bull.*, **15**, 783 (1980).
6. (a) M. M. Thackeray, W. I. F. David, P. G. Bruce, and J. B. Goodenough, *MRS Bull.*, **18**, 461 (1983); (b) M. M. Thackeray, P. J. Johnson, L. A. de Picciotto, P. G. Bruce, and J. B. Goodenough, *MRS Bull.*, **19**, 179 (1984).
7. T. Nagaura, *JEC Battery Newsletter*, **2** (Mar/Apr 1991).
8. G. T. K. Fey, L. Wu, and J. R. Dahn, *J. Electrochem. Soc.*, **141**, 2279 (1994).
9. C. Sigala, D. Guyomard, A. Verbaere, Y. Piffard, and M Toumoux, *Solid State Ionics*, **81**, 167 (1995).
10. (a) Y. Gao, K. Myrtle, M. Zhang, J. N. Reimers, and J. R. Dahn, *Phys. Rev.*, **B54**, 3878 (1996); (b) Q. Zheng, A. Bonakdarpour, M. Zhang, Y. Gao, and J. R. Dahn, *J. Electrochem. Soc.*, **144**, 205 (1997).
11. Y. Ein-Eli and W. F. Howard, *J. Electrochem. Soc.*, **144**, L205 (1997).
12. Y. Ein-Eli, W. F. Howard, S. H. Lu, S. Mukerjee, J. McBreen, J. T. Vaughey, and M. M. Thackeray, *J. Electrochem. Soc.*, **145**, 1238 (1998).
13. Y. Ein-Eli, S. H. Lu, M. A. Rzeznik, S. Mukerjee, X. Q. Yang, and J. McBreen, *J. Electrochem. Soc.*, **145**, 3383 (1998).
14. W. D. Johnston, R. R. Heikes, and D. Sestrich, *J. Phys. Chem. Solids*, **7**, 1 (1958).
15. K. Amine, H. Tukamoto, H.Yasuda, and Y. Fujita, *J. Electrochem. Soc.*, **143**, 1607 (1996).